Advanced Journal of Chemistry, Section A, 2024, 7(4), 374-385

Advanced Journal of Chemistry, Section A

journal homepage: www.ajchem-a.com

Original Research Article

Exploring the Photocatalytic Activity of Magnesium and Copper-Doped Titanium Dioxide Nano Catalyst through Synthesis and Characterization

Jila Talat Mehrabad, Farzad Arjomandi Rad*

Department of Chemistry, Bonab Branch, Islamic Azad University, Bonab, Iran

ARTICLEINFO

Article history

Received: 04 November 2023
Revised: 23 January 2024
Accepted: 19 February 2024
Available Online: 20 February 2024

Manuscript ID: AJCA-2311-1441
Checked for Plagiarism: **Yes**
Language Editor checked: **Yes**
Editor who approved publication: Editorial board

DOI: **10.48309/AJCA.2024.423541.1441**

KEYWORDS

Co-doping
Orange G
Photodegradation
Sol-gel method
Cu-Mg-TiO_2

ABSTRACT

Pristine TiO_2 nanoparticles, doped with single elements Cu and Mg, were synthesized utilizing the sol-gel process with titanium tetraisopropoxide as the Ti basis. The physicochemical characterizations of the nanoparticles were evaluated using X-ray diffraction (XRD), transmission electron microscopy (TEM), diffuse reflection spectroscopy (DRS), and scanning electron microscopy (SEM). The XRD shapes of the samples did not display isolated peaks of diffraction for Cu or Mg, demonstrating that the metals were well spread on the TiO_2 surface. The DRS analysis uncovered an intriguing finding- the co-doped photocatalyst exhibited a significantly narrower band in comparison to both un-doped and monometallic TiO_2. This intriguing alteration in the absorption band near visible light holds great potential. To further explore its implications, a comprehensive comparison was conducted to evaluate the photocatalytic activity of nanoparticles in degrading orange G solution under visible light. TiO_2 nanoparticles doped with copper and magnesium exhibited significantly higher photocatalytic activity than to Cu/TiO_2, Mg/TiO_2, and pure TiO_2 nanoparticles. The optimal doping levels of copper and magnesium for the synthesis of Cu and Mg/TiO_2 nanoparticles were determined to be 1 and 0.25 mol%, respectively.

GRAPHICALABSTRACT

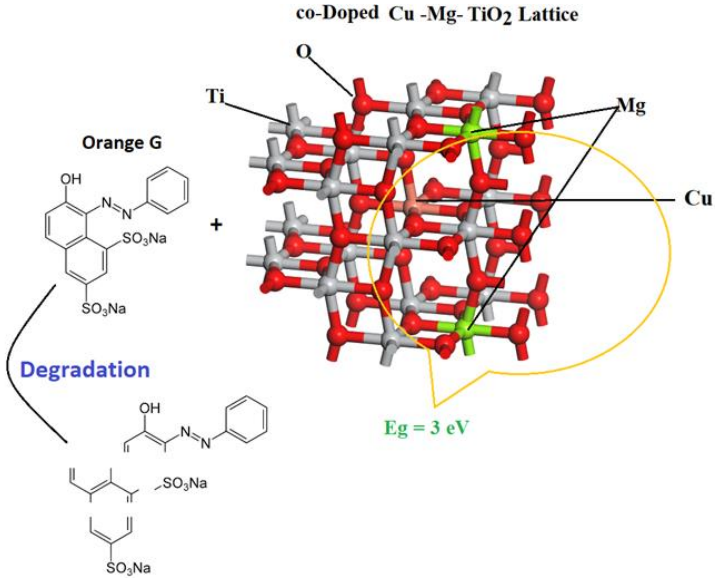

* Corresponding author: Arjomandi Rad, Farzad
✉ E-mail: fdanesh23@gmail.com, f.arjomandirad@bonabiau.ac.ir

Introduction

Various experimental [1] and theoretical [2] techniques are known to remove organic compounds from wastewater. The advanced oxidation process (AOP) could be a broadly used chemical active technique in wastewater treatment. It is highly active in organic compounds removal and has been proposed as a significant technique for eliminating these pollutants from wastewater. The main idea behind enhanced oxidative stress processes is to create hydroxyl radicals (•OH) using substances like H_2O_2, O_3, a photocatalyst, or an oxidant with the help of UV light or sunlight. The hydroxyl radical is a powerful and non-choosy chemical oxidant. Once formed, it starts attacking organic compounds, causing them to break down completely [3]. Heterogeneous photocatalysts like TiO_2 have been widely used due to their excellent performance, lack of toxicity, and easy accessibility. In semiconductor materials, the valence and conduction bands are defined by a bandgap [4]. In the photocatalysis field, the usage of titanium dioxide semiconductor catalysts is more significant than traditional methods for eliminating environmental organic pollutants [5]. This is for the reason that the decomposition of pollutants occurs gradually. Moreover, the catalyst's surface has a strong ability to attract contaminants, allowing the process to continue and terminate even on very small concentrations. This characteristic is of high economic significance [6]. The efficacy of the advanced oxidation progression relies on the stability of the created electron-hole pairs (e-h+). If the e-h+ pair is separated and does not recombine, it can effectively contribute to the decomposition reaction [7]. In laboratory studies, TiO_2 photocatalysts are primarily examined using anatase-phase powder materials. However, it is also common to investigate thin films and rutile materials [8-10]. Anatase phase titanium dioxide (TiO_2) is the chief common photocatalyst because it is a powerful oxidizer and is physically and chemically stable [11-14]. Recently, A.M. Alotaibi *et al.* successfully deposited highly photoactive Cu-doped anatase TiO_2 tinny films on the glass substrate utilizing aerosol-assisted chemical vapor deposition (AACVD) [15]. The photocatalysts activity is less effective for fast recombination of electron-hole pairs. Moreover, the performance may be limited by the relatively small specific surface areas of smooth surfaces and monocrystalline phases [16-19]. Fortunately, it is possible to design and manufacture 1D TiO_2 surface heterostructures that introduce secondary phases with specific morphologies such as nanoparticles, nanorods, and nanowires [20,21]. Moreover, these heterostructures can also incorporate other constituents for example metals, non-metals, and semiconductors through doping [22-24]. There are two primary factors that control the activity of TiO_2 photocatalyst: reducing the bandgap in the visible light region and decreasing the electrons-holes recombination rate. Doping is a method to overcome this limitation [25]. TiO_2 doping with certain elements can decrease the bandgap, which in turn moves to the visible range of the absorption band. There are several techniques for doping TiO_2, such as ion implantation, hydrothermal reaction, sol-gel reaction, and solid-state reaction [26-29]. The sol-gel technique is considered the easiest, most cost-effective, and appealing way to synthesize titanium dioxide and metal doping at low temperatures. In recent years, numerous researchers have focused on encoding TiO_2 to address these issues. R. Lakshmi *et al.* have confirmed that the addition of Co and Fe to TiO_2 powder, obtained through the sol-gel process, enhances its photocatalytic activity for decomposing the main dye malachite green. This activity is higher compared to single metal and undoped TiO_2 [30].

Recently, there have been reports about the production of TiO_2-bimetallic sol-gels using co-

doped particles such as Ni-Ag / TiO_2 [31], Cu-Zn / TiO_2 [32], and Pd-Ag/ TiO_2 [33]. There are various regulations for mono non-metal [34] and mixed element doping, which include non-metal doping [35-38] and doping of transition metal [39-41]. Doping of the transition elements can significantly progress the photocatalytic activity in a range of visible light [42]. Yi-nan Wu *et al.* conducted a study where they used leaf extract of Stephania abyssinica with (Mn, Ni) co-doped ZnO catalysts. They also evaluated the photocatalyst activity by testing its capability to decompose the methylene blue (MB) dye under visible light [43]. A recent study examined a new method for analyzing the methyl orange degradation using a modified TiO_2 nanocomposite. The study found that the efficacy of removing methyl orange rises with longer irradiation of UV light and a higher weight fraction [44].

Therefore, in this study, we prepared nanoparticles of TiO_2, Cu/TiO_2, Mg/TiO_2, and bimetallic Cu, Mg/TiO_2, and then evaluation the comparative activity of above photocatalysts in removing Orange G is accomplished. To understand the structural properties of the catalysts, we used techniques such as X-ray diffraction (XRD), scanning electron microscopy (SEM), energy dispersive X-ray spectroscopy (EDX), transmission electron microscopy (TEM), and UV-Vis diffuse reflectance spectroscopy (DRS).

Experimental

Materials and methods

Copper nitrate and magnesium nitrate hexahydrate were utilized as metal salts for doping. Titanium tetraisopropoxide (Ti $(OC_3H_7)_4$) was applied as the predecessor for titania. Methanol (MeOH) with a purity of 96% was used, and Orange G was chosen as the azo dye model for the study on photocatalytic decomposition. All materials were prepared from Merck, Germany. The chemical structure of Orange G is displayed in Figure 1.

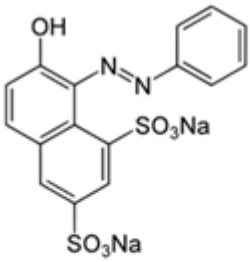

Chemical formula $C_{16}H_{10}N_2Na_2O_7S_2$

M_W (g mol^{-1}) : 452.38 $gmol^{-1}$

Figure 1. Chemical structure and characteristics of Orange G.

TiO_2 and doped TiO_2 nanoparticles synthesis with the sol-gel process

Nano-TiO_2, sole-doped, and Cu/Mg co-doped nano-TiO_2 nanoparticles were produced using the sol-gel method with titanium isopropoxide (TTIP) as the pioneer for TiO_2. To prepare the co-doped TiO_2 samples, the molar ratio of TTIP, methanol, and distilled water was maintained at 1:1:65. TTIP was dissolved in methanol and the time of sonication was for 20 minutes. Distilled water was then added gradually to the solution while vigorously stirring, and the mixture was refluxed for 3 hours to produce a white suspension. The mixed solution was stirred for 1 hour after adding appropriate amounts of Mg $(NO_3)_2$ and Cu $(NO_3)_2$. The final solution was then dried in a furnace at 100 °C for twelve hours and calcined at 455 °C in the furnace for 4 hours to prepare Nano-Cu, Mg/TiO_2. Monometallic and pure (anatase) TiO_2 were also prepared using a similar process.

Characterization

XRD patterns were obtained to identify phases and calculate crystallite size. The patterns were proved by a Siemens D5000 X-ray diffractometer

by Cu-Kα radiation, with measurements taken in the 2θ range of 20-80°. The average crystallinity size (D_{nm}) was determined by equation of Scherrer, as described in Equation (5) [45];

$$D = k\lambda/\beta \cos\theta \quad (5)$$

In this equation, we have several variables: k, λ, β, and θ. The constant k is alike to 0.89. The wavelength of X-ray, λ, is alike to 0.154056 nm. The variable β represents the full width at half maximum intensity (FWHM). Recently, θ is the half diffraction angle. The catalyst's optical bandgap (Eg) was measured by an Avaspec-2048 TEC spectrometer to quantity the DRS of the samples. The bandgap energies of all the samples were determined with the following Equation (6):

$$E_g\ (eV) = 1240/\lambda\ (nm) \quad (6)$$

The chemical structure of the catalyst that was prepared was analyzed using the EDX system. To observe the catalyst at a microscopic level, a Philips CM-10 HT-100 keV electron microscope was used for TEM observations. In addition, SEM analysis was conducted on the samples coated with gold using a Philips model XL30 instrument.

Photocatalytic decomposition activity of the samples

The photocatalytic decomposition process was conducted in a batch quartz reactor. In the experimentation, 40 mg of the photocatalyst was mixed to 100 mL of distilled water. In an ultrasonic bath at 25 °C, the mixture was sonicated for 15 minutes. After that, Orange G was added to the mixture, reaching a last concentration of 20 mg L^{-1} and a volume of 100 mL. The mixture was stirred in the dark for 30 minutes to guarantee that the adsorption balance was reached. Samples of 7 mL were placed at specific interludes of irradiation time. These samples were centrifuged twofold for 15 minutes each time to remove any suspended solid photocatalyst.

Finally, the samples were evaluated with a UV-Vis spectrophotometer (UV-Shimadzu 2100).

Results and Discussion

Structural analysis

X-ray diffraction (XRD) study of prepared photocatalysts

Figure 2 displays the XRD shapes of Cu/TiO_2 (1 mol%), Mg/TiO_2 (0.25 mol%), and $Cu, Mg/TiO_2$ (1-0.25 mol%) after being heated to 450 °C. The XRD pattern in the figure comprises primarily anatase with a slight quantity of rutile phase (80:20 ratio). All the photocatalysts display prominent anatase phase peaks at 2θ = 25.2, 38, 48.2, 55, and 62.5 degrees, along with a little portion of rutile phase peaks at 2θ = 32 and 70 grades. The middle size of the crystallites is calculated using the Debye-Scherrer equation, and it is around 50 nm for all the samples. There are no noticeable distinctions in the crystallite dimensions and crystal construction of the samples after the addition of Cu and Mg.

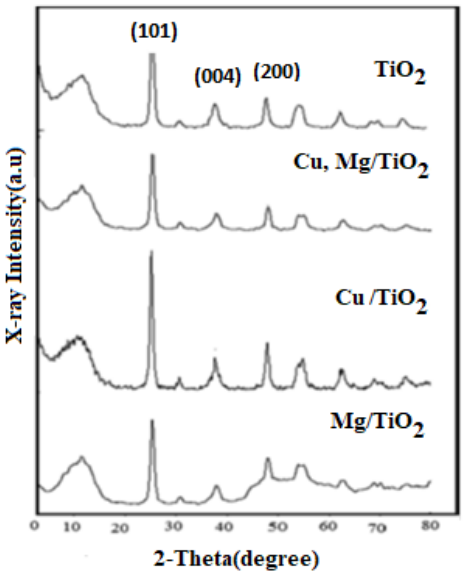

Figure 2. The XRD shapes of TiO_2, Cu/TiO_2 (1 mol%), Mg/TiO_2 (0.25 mol%) and $Cu, Mg/TiO_2$ (1-0.25 mol%) calcined at 450 ˚C

When comparing un-doped TiO_2 nanoparticles, the diffraction intensity peak (101 plane) of Cu, Mg/TiO_2 nanoparticles, and Cu/TiO_2 increased significantly. This can be credited to the smaller ionic radius of Cu^{2+} (0.073 nm) being introduced into the larger ionic radii of Ti^{4+} (0.074 nm) [46].

Analysis of transmission electron microscopy (TEM)

To investigate the part size, the transmission electron microscope was used to capture images of the Cu and Mg/TiO_2 nanoparticles (Figure 3).

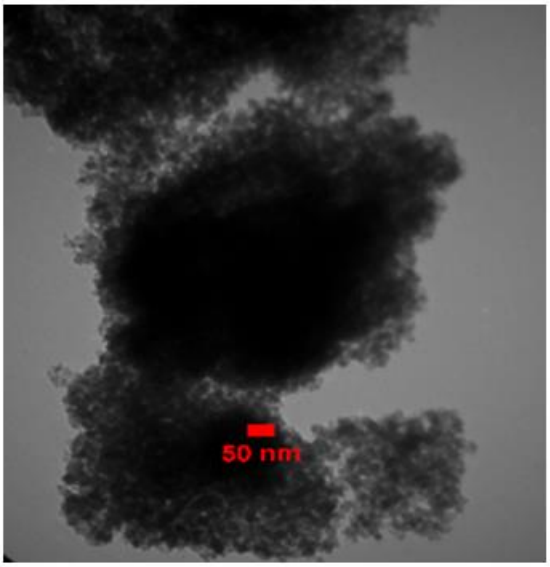

Figure 3. The TEM image of Cu and Mg/TiO_2 calcined at 450 °C

The sizes of these nanoparticles were consistent with the sizes of the crystals achieved by the XRD patterns.

Examination of scanning electron microscopy (SEM)

The SEM was applied to syudy the structure of the doped TiO_2 nanoparticles. Figure 4 demonstrates an SEM image of TiO_2 that was co-doped with Cu and Mg and then heated to 450 °C. The particles are evenly spread out, the structure is compact, the uniformity is excellent, the shape is round, and there are only a few clumps.

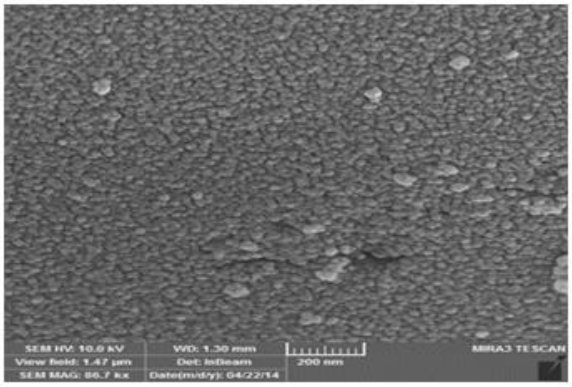

Figure 4. SEM of Cu, Mg/TiO_2 calcined at 450 °

Diffuse reflectance spectroscopy (DRS) analysis

The DRS technique was exploited to investigate how the addition of Cu and Mg affects the TiO_2 bandgap. Both the size of the grains and the defects in the crystal lattice of TiO_2 show a noteworthy role in determining the bandgap energy values of TiO_2 [47]. Figure 5 illustrates the optical absorption property of TiO_2, Mg/TiO_2, Cu/TiO_2, and Cu, Mg/TiO_2 nanoparticles. Table 1 presents the bandgap energies of all the samples. The TiO_2, co-doped with Cu and Mg, exhibits a noticeable change in the absorption peak within the visible light scale of 400-900 nm. This shift is attributed to the combined effect of magnesium and copper, which creates additional absorption peaks that extend beyond the bandgap.

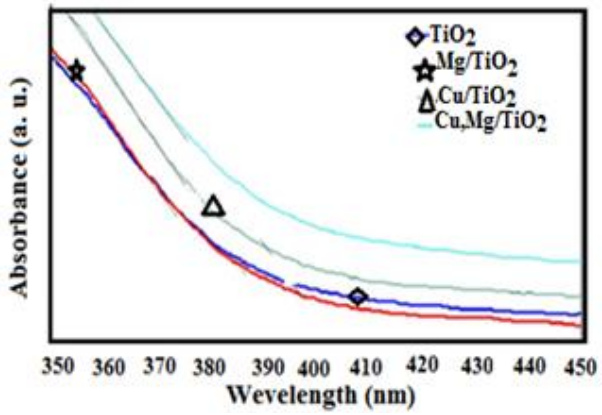

Figure 5. Examining the TiO_2, Mg/TiO_2, Cu $/TiO_2$, and Cu, Mg/TiO_2 nanoparticles involved conducting DRS-UV-Vis spectroscopy [48]

Studies of photocatalytic activity

Efficiency of Cu and Mg doping

The reaction rate constants (k_{ap}) for removing Orange G through photocatalysis were determined by analyzing the slant of the semi-logarithmic diagrams. Table 2 sumarizes the k_{ap} values obtained for the removal of Orange G using different types of nanoparticles, including Cu/TiO_2, Mg/TiO_2, and Cu, Mg/TiO_2. According to the findings, the k_{ap} value increased as the Cu loading reached up to 1 mol%. In the process of photocatalysis, Cu serves as a bowl for charge carriers generated by light, which helps facilitate the transfer of charges at the boundary and prevents the electron-hole pairs recombination.

Table 1. E_g values of monometallic and bimetallic Cu and Mg-doped TiO_2 nanoparticle

Catalyst	λ_{max} (nm)	E_g (eV)
TiO_2	392	3.61
Cu/TiO_2	395	3.42
Mg/TiO_2	391	3.52
Cu Mg/TiO_2	406	3.00

This is because Cu has a strong capability to trap electrons, thereby enhancing the photocatalysis effectiveness. Based on Table 2, the highest activity of photocatalytic for Mg-doped TiO_2 nanoparticles was achieved when the Mg content was 0.25 mol%. This is probably because the increased concentration of the dopant leads to a greater number of charge carriers being trapped per particle. However, when there is an excessive amount of Mg on the exterior of TiO_2, it becomes the main center for the electron-hole pairs recombination generated during photocatalysis. This inhibits the transfer of electrons and holes at the border, lead to a decrease in photoactivity [49].

Catalyst dosage effect

A set of experiments were conducted to investigate the impact of catalyst quantity on the degradation of orange G and identify the most effective dosage by testing different levels of co-doped nano-TiO_2, ranging from 200 to 600 mg L^{-1}, in 100 mL of Orange G solution with a concentration of 20 ppm. Figure 6 illustrates the distinction of the pseudo-first-order rate constants for four various catalyst doses below visible light. The rate of degradation originated to improve as the catalyst amount increased up to 400 mg L^{-1}.

However, a degradation rate reduction was detected when the catalyst amount exceeded 400 mg L^{-1}. When the dose of Cu, Mg- doped TiO_2 augmented, there was an increase in the quantity of absorbed photons and dye molecules adsorption compared to the rise in catalyst molecules. This trend continued until the active surface area reached a constant level. When there is too much catalyst because light cannot penetrate well and scattering of light increases, the ability to remove orange G through photocatalysis will decrease [50].

Photocatalytic activity comparison of TiO_2, Mg/TiO_2, Cu/TiO_2, and Cu, Mg/TiO_2

Figure 7 presents a comparison of the nanoparticle's efficiency of pure, monometallic, and bimetallic co-doped TiO_2 in removing Orange G through photocatalysis underneath visible light.

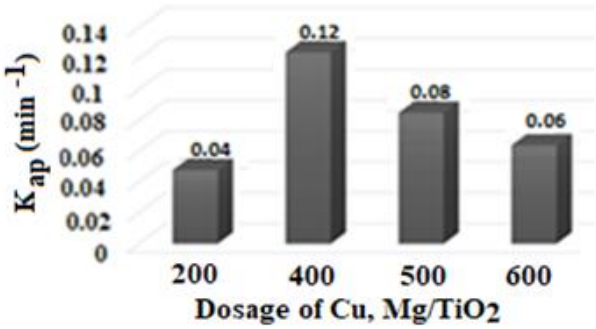

Figure 6. Effect of several dosages of Cu and Mg/TiO_2 nanoparticles at the Orange G degradation

Table 2. The apparent reaction rate constant (k_{ap}) of dissimilar catalysts in the process of photocatalytic decomposition of orange G

Catalyst	Doping of Metal (mol%) Cu	Mg	Calcination Temperature (°C)	k_{ap}(min $^{-1}$)
TiO_2	0.0	0.0	400	0.0490
Mg/TiO_2	0.0	0.25	400	0.0551
Cu/TiO_2	0.01	0.0	400	0.0488
Cu /TiO_2	0.05	0.0	400	0.0523
Cu /TiO_2	1.0	0.0	450	0.0710
Cu /TiO_2	0.15	0.0	400	0.0585
Cu, Mg/TiO_2	1.0	0.15	400	0.0723
Cu, Mg/TiO_2	1.0	0.25	400	0.1122
Cu, Mg/TiO_2	1.0	0.5	400	0.0971
Cu, Mg/TiO_2	1.0	1.0	400	0.0613
Cu, Mg/TiO_2	1.0	0.25	300	0.0871
Cu, Mg/TiO_2	1.0	0.25	500	0.0751
Cu, Mg/TiO_2	1.0	0.25	600	0.0488

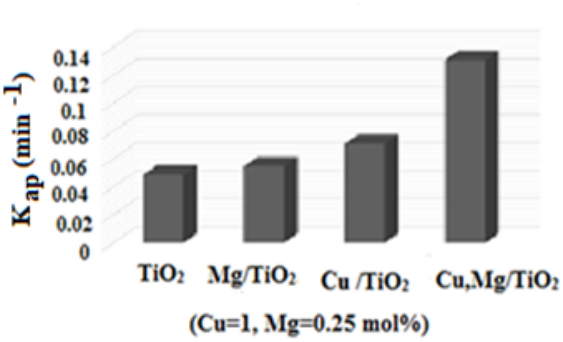

Figure 7. Comparative examine between the photocatalytic activeness of TiO_2, Mg/TiO_2, Cu /TiO_2, and Cu, Mg/TiO_2

The results indicate that Cu and Mg/TiO_2 nanoparticles exhibit the maximum photocatalytic action. This improvement can be credited to the ability of copper and magnesium to increase surface area, and visible light absorption, enhance the separation of photogenerated electron-hole pairs, increase active sites [51], capture electrons generated by light, and prevent their recombination with holes, thus enhancing the photocatalytic process.

Furthermore, the co-doped catalyst exhibits superior photocatalytic performance related to its bigger surface zone.

The effectiveness of calcination temperature

To examine how the temperature at which a catalyst is calcined affects its photocatalytic activity, Mg (0.25 mol%) and Cu (1mol%) were calcined at 300, 400, 500, and 600 °C for 3 hours.

Figure 8 shows that the calcination temperature has a noteworthy impact on the photocatalytic activity of the co-doped TiO_2 nanoparticles. As the temperature rises, the transition from amorphous to anatase form of TiO_2 increases. Anatase TiO_2 exhibits higher photocatalytic activity, resulting in a gradual increase in photocatalytic activity.

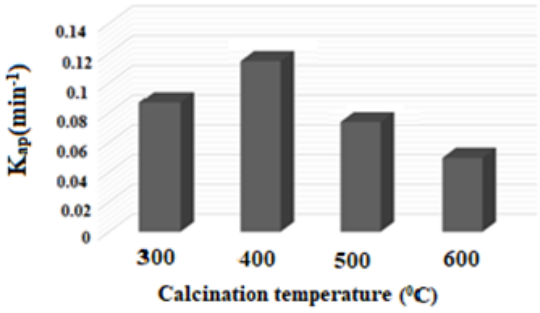

Figure 8. The effectiveness of optimum calcination temperature on the degradation of Orange G under visible light radiation and the photocatalytic activity of Cu, Mg/TiO_2 nanoparticles.

However, if the calcination temperature exceeds 400 °C, TiO_2 can convert from anatase to rutile form and the particle size will increase with higher temperatures.

This can be attributed to some factors, counting the agglomeration of the nanoparticles, a decrease in the amount of H_2O adsorbed, growth in the rate of recombination between e- and h+, and the conversion of anatase to the rutile phase, which has lower photocatalytic activity [52].

Investigating the effect of pH on the removal rate of Orange G with optimal amounts of Cu, Mg-TiO_2

At this stage of the research, solutions containing 20 mg L^{-1} of Orange G and with the optimal amount of Cu, Mg-TiO_2 photocatalyst (400 mg L^{-1}) were prepared and the color removal was investigated at different pHs at specific time intervals (Figure 9). The rate of degradation in acidic pH is higher than in alkaline pH. The high degradation rate constant in acidic pH is due to the increase of surface absorption of Orange G in the nanoparticle surface area. In addition, minimizing electron-hole recombination in acidic pH is another important factor for constant increase in degradation rate. At high pH, repulsion is created between the anionic surface of the dye and the hydroxyl anions, and there is no more chance to react with the dye molecules. Therefore, destruction efficiency decreases.

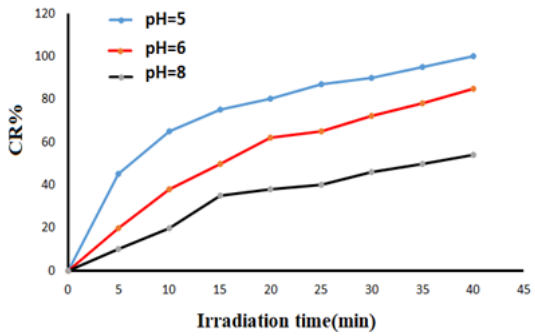

Figure 9. Percentage removal orange G by irradiation time at different pH

Conclusion

This finding suggests that the co-doped TiO_2 nanoparticles made of copper and magnesium with the sol-gel method enhanced the photocatalytic activity in comparison with the single-metal TiO_2 nanoparticles. The addition of Cu and Mg to TiO_2 prevents the transition of phase from anatase to rutile at optimal temperatures, which is crucial for maintaining the desired photocatalytic properties. The XRD standard analysis confirms that the co-doped TiO_2 nanoparticles retain their anatase phase even at 400 °C, whereas uncoated single-metal TiO_2 nanoparticles undergo a phase change to rutile. This is significant because the anatase phase of TiO_2 is known to possess superior photocatalytic activity compared to rutile. In addition, the co-doping strategy allowed for fine-tuning of the photocatalytic properties by adjusting the concentration of copper and magnesium ions. By optimizing their ratios, it was possible to achieve the maximum photocatalytic activity while maintaining phase stability.

Acknowledgements

Maragheh Islamic Azad University Chemistry Research Laboratory, which supported part of the devices and raw materials of this project.

Disclosure statement

The authors declares that there is no conflict of interest in this study.

Orcid

Jila Talat Mehrabad: 0000-0002-5866-8973
Farzad Arjomandi Rad: 0000-0002-4864-5831

References

[1] R. Rahimian, S. Zarinabadi, A review of studies on the removal of methylene blue dye from industrial wastewater using activated carbon adsorbents made from almond bark, *Progress in Chemical and Biochemical Research*, **2020**, *3*, 251-268. [Google Scholar], [Publisher]

[2] S. Armaković, S. Armaković, Computational studies of stability, reactivity and degradation properties of ephedrine; a stimulant and precursor of illicit drugs, *Advanced Journal of Chemistry-Section B*, **2020**, *2*, 73-80. [Google Scholar], [Publisher]

[3] A. Kurt, B.K. Mert, N. Özengin, Ö. Sivrioğlu, T. Yonar, Treatment of antibiotics in wastewater using advanced oxidation processes (AOPs), *Physico-chemical Wastewater Treatment and Resource Recovery*, **2017**, *175*. [Google Scholar], [Publisher]

[4] M.H. Mahdi, T.J. Mohammed, J. Al-Najar, Advanced Oxidation Processes (AOPs) for treatment of antibiotics in wastewater: a review, *IOP Conference Series: Earth and Environmental Science, IOP Publishing*, **2021**, 012109. [CrossRef], [Google Scholar], [Publisher]

[5] F. Ghanaat, L. Vafajoo, M. Haddadi, Affecting Parameters on Photocatalytic Degradation of Organic Contaminants in a Synthesized Wastewater Utilizing Concentrated Solar UV, *Progress in Chemical and Biochemical Research*, **2022**, *5*, 331-337. [CrossRef], [Google Scholar], [Publisher]

[6] H. Hao, J.L. Shi, H. Xu, X. Li, X. Lang, N-hydroxyphthalimide-TiO2 complex visible light photocatalysis, *Applied Catalysis B: Environmental*, **2019**, *246*, 149-155. [CrossRef], [Google Scholar], [Publisher]

[7] S. Abbasi, The degradation rate study of methyl orange using MWCNTs@ TiO2 as photocatalyst, application of statistical analysis based on Fisher's F distribution, *Journal of cluster science*, **2022**, *33*, 593-602. [CrossRef], [Google Scholar], [Publisher]

[8] D. Hanaor, G. Triani, C.C. Sorrell, Morphology and photocatalytic activity of highly oriented mixed phase titanium dioxide thin films, *Surface and Coatings Technology*, **2011**, *205*, 3658-3664. [CrossRef], [Google Scholar], [Publisher]

[9] D.A. Hanaor, C.C. Sorrell, Sand Supported Mixed-P hase Ti O 2 Photocatalysts for Water Decontamination Applications, *Advanced Engineering Materials*, **2014**, *16*, 248-254. [CrossRef], [Google Scholar], [Publisher]

[10] J. Schneider, M. Matsuoka, M. Takeuchi, J. Zhang, Y. Horiuchi, M. Anpo, D.W. Bahnemann, Understanding TiO2 photocatalysis: mechanisms and materials, *Chemical Reviews*, **2014**, *114*, 9919-9986. [CrossRef], [Google Scholar], [Publisher]

[11] R.A. Carcel, L. Andronic, A. Duta, Photocatalytic activity and stability of TiO2 and WO3 thin films, *Materials Characterization*, **2012**, *70*, 68-73. [CrossRef], [Google Scholar], [Publisher]

[12] A. Fujishima, K. Honda, Electrochemical photolysis of water at a semiconductor electrode, *Nature*, **1972**, *238*, 37-38. [CrossRef], [Google Scholar], [Publisher]

[13] L. Mino, C. Negri, R. Santalucia, G. Cerrato, G. Spoto, G. Martra, Morphology, surface structure and water adsorption properties of TiO2 nanoparticles: a comparison of different commercial samples, *Molecules*, **2020**, *25*, 4605. [CrossRef], [Google Scholar], [Publisher]

[14] V. Augugliaro, M. Bellardita, V. Loddo, G. Palmisano, L. Palmisano, S. Yurdakal, Overview on oxidation mechanisms of organic compounds by TiO2 in heterogeneous photocatalysis, *Journal of Photochemistry and Photobiology C: Photochemistry Reviews*, **2012**, *13*, 224-245. [Crossref], [Google Scholar], [Publisher]

[15] A.M. Alotaibi, B.A. Williamson, S. Sathasivam, A. Kafizas, M. Alqahtani, C. Sotelo-Vazquez, J.

Buckeridge, J. Wu, S.P. Nair, D.O. Scanlon, Enhanced photocatalytic and antibacterial ability of Cu-doped anatase TiO2 thin films: theory and experiment, *ACS Applied Materials & Interfaces*, **2020**, *12*, 15348-15361. [CrossRef], [Google Scholar], [Publisher]

[16] A.N. Banerjee, The design, fabrication, and photocatalytic utility of nanostructured semiconductors: focus on TiO2-based nanostructures, *Nanotechnology, Science and Applications*, **2011**, 35-65. [Google Scholar], [Publisher]

[17] Y. Lai, L. Wang, D. Liu, Z. Chen, C. Lin, TiO2-Based nanomaterials: design, synthesis, and applications, *Journal of Nanomaterials*, **2015**, *2015*, 5-5. [CrossRef], [Google Scholar], [Publisher]

[18] W. Zhou, H. Liu, R.I. Boughton, G. Du, J. Lin, J. Wang, D. Liu, One-dimensional single-crystalline Ti–O based nanostructures: properties, synthesis, modifications and applications, *Journal of Materials Chemistry*, **2010**, *20*, 5993-6008. [CrossRef], [Google Scholar], [Publisher]

[19] J. Zhang, F.X. Xiao, G. Xiao, B. Liu, Self-assembly of a Ag nanoparticle-modified and graphene-wrapped TiO 2 nanobelt ternary heterostructure: surface charge tuning toward efficient photocatalysis, *Nanoscale*, **2014**, *6*, 11293-11302. [CrossRef], [Google Scholar], [Publisher]

[20] K. Pan, Y. Dong, C. Tian, W. Zhou, G. Tian, B. Zhao, H. Fu, TiO2-B narrow nanobelt/TiO2 nanoparticle composite photoelectrode for dye-sensitized solar cells, *Electrochimica Acta*, **2009**, *54*, 7350-7356. [CrossRef], [Google Scholar], [Publisher]

[21] M.A. Hossain, J. Park, J.Y. Ahn, C. Park, Y. Kim, S.H. Kim, D. Lee, Investigation of TiO2 nanotubes/nanoparticles stacking sequences to improve power conversion efficiency of dye-sensitized solar cells, *Electrochimica Acta*, **2015**, *173*, 665-671. [CrossRef], [Google Scholar], [Publisher]

[22] Z. Győri, Z. Kónya, Á. Kukovecz, Visible light activation photocatalytic performance of PbSe quantum dot sensitized TiO2 Nanowires, *Applied Catalysis B: Environmental*, **2015**, *179*, 583-588. [CrossRef], [Google Scholar], [Publisher]

[23] S.H. Ahn, W.S. Chi, J.T. Park, J.K. Koh, D.K. Roh, J.H. Kim, Direct assembly of preformed nanoparticles and graft copolymer for the fabrication of micrometer-thick, organized TiO2 films: high efficiency solid-state dye-sensitized solar cells, *Advanced Materials (Deerfield Beach, Fla.)*, **2011**, *24*, 519-522. [CrossRef], [Google Scholar], [Publisher]

[24] M.Z. Ge, C.Y. Cao, J.Y. Huang, S.H. Li, S.N. Zhang, S. Deng, Q.S. Li, K.Q. Zhang, Y.K. Lai, Synthesis, modification, and photo/photoelectrocatalytic degradation applications of TiO2 nanotube arrays: a review, *Nanotechnology Reviews*, **2016**, *5*, 75-112. [CrossRef], [Google Scholar], [Publisher]

[25] C.M. Whang, J. Kim, H.J. Hwang, Photocatalytic properties of the transition metal doped TiO2 powder prepared by sol-gel process, *Key Engineering Materials*, **2004**, *280*, 647-650. [CrossRef], [Google Scholar], [Publisher]

[26] U. Akpan, B. Hameed, The advancements in sol–gel method of doped-TiO2 photocatalysts, *Applied Catalysis A: General*, **2010**, *375*, 1-11. [CrossRef], [Google Scholar], [Publisher]

[27] E. Jeong, P.H. Borse, J. Jang, J. Lee, O.S. Jung, H. Chang, J. Jin, M. Won, H. Kim, Hydrothermal synthesis of Cr and Fe co-doped TiO2 nanoparticle photocatalyst, *Journal of Ceramic Processing Research*, **2008**, *9*, 250-253. [Google Scholar], [Publisher]

[28] D.H. Kim, S. Woo, S. Moon, H. Kim, B. Kim, J. Cho, Y. Joh, E. Kim, Effect of Co/Fe co-doping in TiO2 rutile prepared by solid state reaction, *Solid State Communications*, **2005**, *136*, 554-558. [CrossRef], [Google Scholar], [Publisher]

[29] X. Chen, S.S. Mao, Titanium dioxide nanomaterials: synthesis, properties,

modifications, and applications, *Chemical reviews*, **2007**, *107*, 2891-2959. [CrossRef], [Google Scholar], [Publisher]

[30] R.L. Narayana, M. Matheswaran, A. Abd Aziz, P. Saravanan, Photocatalytic decolourization of basic green dye by pure and Fe, Co doped TiO2 under daylight illumination, *Desalination*, **2011**, *269*, 249-253. [CrossRef], [Google Scholar], [Publisher]

[31] H.Y. Chuang, D.H. Chen, Fabrication and photocatalytic activities in visible and UV light regions of Ag@ TiO2 and NiAg@ TiO2 nanoparticles, *Nanotechnology*, **2009**, *20*, 105704. [CrossRef], [Google Scholar], [Publisher]

[32] D. Zhang, F. Zeng, Photocatalytic oxidation of organic dyes with visible-light-driven codoped TiO 2 photocatalysts, *Russian Journal of Physical Chemistry A*, **2011**, *85*, 1077-1083. [CrossRef], [Google Scholar], [Publisher]

[33] K. Kontapakdee, J. Panpranot, P. Praserthdam, Effect of Ag addition on the properties of Pd–Ag/TiO2 catalysts containing different TiO2 crystalline phases, *Catalysis Communications*, **2007**, *8*, 2166-2170. [CrossRef], [Google Scholar], [Publisher]

[34] F.A. Rad, J.T. Mehrabad, M.D. Esrafili, A Communal Experimental and DFT Study on Structural and Photocatalytic Properties of Nitrogen-Doped TiO2, **2023**, *6*, 244-252. [CrossRef], [Google Scholar], [Publisher]

[35] R. Asahi, T. Morikawa, T. Ohwaki, K. Aoki, Y. Taga, Visible-light photocatalysis in nitrogen-doped titanium oxides, *science*, **2001**, *293*, 269-271. [CrossRef], [Google Scholar], [Publisher]

[36] H. Irie, Y. Watanabe, K. Hashimoto, Nitrogen-concentration dependence on photocatalytic activity of TiO2-x N x powders, *The Journal of Physical Chemistry B*, **2003**, *107*, 5483-5486. [CrossRef], [Google Scholar], [Publisher]

[37] S.U. Khan, M. Al-Shahry, W.B. Ingler Jr, Efficient photochemical water splitting by a chemically modified n-TiO2, *science*, **2002**, *297*, 2243-2245. [CrossRef], [Google Scholar], [Publisher]

[38] J. Xu, Y. Ao, D. Fu, C. Yuan, Synthesis of fluorine-doped titania-coated activated carbon under low temperature with high photocatalytic activity under visible light, *Journal of Physics and Chemistry of Solids*, **2008**, *69*, 2366-2370. [CrossRef], [Google Scholar], [Publisher]

[39] T.L. Thompson, J.T. Yates, Surface science studies of the photoactivation of TiO2 new photochemical processes, *Chemical reviews*, **2006**, *106*, 4428-4453. [CrossRef], [Google Scholar], [Publisher]

[40] R. Khan, S.W. Kim, T.J. Kim, C.M. Nam, Comparative study of the photocatalytic performance of boron–iron Co-doped and boron-doped TiO2 nanoparticles, *Materials Chemistry and Physics*, **2008**, *112*, 167-172. [CrossRef], [Google Scholar], [Publisher]

[41] S. Buddee, S. Wongnawa, U. Sirimahachai, W. Puetpaibool, Recyclable UV and visible light photocatalytically active amorphous TiO2 doped with M (III) ions (M= Cr and Fe), *Materials Chemistry and physics*, **2011**, *126*, 167-177. [CrossRef], [Google Scholar], [Publisher]

[42] Q. Meng, T. Wang, E. Liu, X. Ma, Q. Ge, J. Gong, Understanding electronic and optical properties of anatase TiO 2 photocatalysts co-doped with nitrogen and transition metals, *Physical Chemistry Chemical Physics*, **2013**, *15*, 9549-9561. [CrossRef], [Google Scholar], [Publisher]

[43] H.H. Haitosa, B.B. Tesfamariam, N.S. Gultom, D.H. Kuo, X. Chen, Y.n. Wu, O.A. Zelekew, Stephania abyssinica leaf extract mediated (Mn, Ni) co-doped ZnO catalyst synthesis for the degradation of organic dye, *Journal of Molecular Liquids*, **2022**, *368*, 120666. [CrossRef], [Google Scholar], [Publisher]

[44] S. Abbasi, M. Hasanpour, F. Ahmadpoor, M. Sillanpää, D. Dastan, A. Achour, Application of the statistical analysis methodology for

photodegradation of methyl orange using a new nanocomposite containing modified TiO2 semiconductor with SnO2, *International journal of environmental analytical chemistry*, **2021**, *101*, 208-224. [CrossRef], [Google Scholar], [Publisher]

[45] F.T.L. Muniz, M.R. Miranda, C. Morilla dos Santos, J.M. Sasaki, The Scherrer equation and the dynamical theory of X-ray diffraction, *Acta Crystallographica Section A: Foundations and Advances*, **2016**, *72*, 385-390. [CrossRef], [Google Scholar], [Publisher]

[46] W. Guan, F. Ji, Z. Xie, R. Li, N. Mei, Preparation and photocatalytic performance of nano-TiO2 codoped with iron III and lanthanum III, *Journal of Nanomaterials*, **2015**, *2015*, 4-4. [CrossRef], [Google Scholar], [Publisher]

[47] M.A. Behnajady, H. Eskandarloo, Characterization and photocatalytic activity of Ag–Cu/TiO2 nanoparticles prepared by sol–gel method, *Journal of Nanoscience and Nanotechnology*, **2013**, *13*, 548-553. [CrossRef], [Google Scholar], [Publisher]

[48] F. Arjomandi Rad, J. Talat Mehrabad, R. Khalilnezhad, Investigation of Photocatalytic Activity of Acid Red 27 by Co-doped TiO2 Nanoparticle with Magnesium and Copper, *Journal of Environmental Science and Technology*, **2021**, *23*, 17-26. [Google Scholar]

[49] S. Ahmed, M. Rasul, W.N. Martens, R. Brown, M. Hashib, Heterogeneous photocatalytic degradation of phenols in wastewater: a review on current status and developments, *Desalination*, **2010**, *261*, 3-18. [CrossRef], [Google Scholar], [Publisher]

[50] C. Wong, W. Chu, The direct photolysis and photocatalytic degradation of alachlor at different TiO2 and UV sources, *Chemosphere*, **2003**, *50*, 981-987. [CrossRef], [Google Scholar], [Publisher]

[51] A. Abutaleb, Synthesis of Copper/Sulfur Co-Doped TiO2-Carbon Nanofibers as Catalysts for H2 Production via NaBH4 Hydrolysis, *Inorganics*, **2023**, *11*, 352. [CrossRef], [Google Scholar], [Publisher]

[52] M. Behnajady, H. Eskandarloo, N. Modirshahla, M. Shokri, Investigation of the effect of sol–gel synthesis variables on structural and photocatalytic properties of TiO2 nanoparticles, *Desalination*, **2011**, *278*, 10-17. [CrossRef], [Google Scholar], [Publisher]

HOW TO CITE THIS ARTICLE

Jila Talat Mehrabad, Farzad Arjomandi Rad. Exploring the Photocatalytic Activity of Magnesium and Copper-Doped Titanium Dioxide Nano Catalyst through Synthesis and Characterization. *Adv. J. Chem. A*, 2024, 7(4), 374-385.

DOI: 10.48309/AJCA.2024.423541.1441
URL: https://www.ajchem-a.com/article_190643.html